metals

MDPI

Article

Study on the Subcritical Quenching Process of High-Chromium Cast Iron Prepared by Squeeze Casting

Aili Shan, Shuming Xing *, Biwei Zhao, Wenjing Gao, Tong Wu and Hongji Sun

School of Mechanical and Electronic Control Engineering, Beijing Jiaotong University, Beijing 100044, China
* Correspondence: smxing@bjtu.edu.cn; Tel.: +86-136-4115-6691

Abstract: In this study, the heat treatment process of a high-chromium cast iron (HCCI) alloy prepared via 128 MPa squeeze casting at different subcritical quenching temperatures was investigated. The results showed that subcritical heat treatment can change the martensite content, the carbide type and size of the squeeze casting HCCI microstructure. Furthermore, it was revealed that the subcritical quenching heat treatment can improve the hardness of the liquid-forged HCCIs. When the quenching temperature increased from 500 °C to 530 °C, the hardness of the alloy increased significantly, reaching a maximum value of 57 HRC. Thereafter, if the temperature continued to rise to 630 °C, the hardness decreased rapidly. For impact toughness, when the quenching temperature was 500 °C, the toughness of alloy increased by 0.9 J/cm^2 than that of the no heat treatment group. If the quenching temperature continued to increase, the toughness was reduced. Taking hardness and toughness into account, the microstructure evolution diagram of the optimal process-500 °C subcritical quenching process was established, various characterisation techniques were used to gain insights into the optimal heat treatment process. Compared with high temperature heat treatment, subcritical heat treatment can improve the performance of the HCCI alloy and reduce costs.

Keywords: squeeze casting; subcritical quenching; HCCI; microstructure; hardness; impact toughness

check for updates

Citation: Shan, A.; Xing, S.; Zhao, B.; Gao, W.; Wu, T.; Sun, H. Study on the Subcritical Quenching Process of High-Chromium Cast Iron Prepared by Squeeze Casting. *Metals* **2023**, *13*, 570. https://doi.org/10.3390/met13030570

Academic Editor: Nikki Stanford

Received: 10 February 2023
Revised: 6 March 2023
Accepted: 9 March 2023
Published: 12 March 2023

Copyright: © 2023 by the authors. Licensee MDPI, Basel, Switzerland. This article is an open access article distributed under the terms and conditions of the Creative Commons Attribution (CC BY) license (https://creativecommons.org/licenses/by/4.0/).

1. Introduction

HCCI (with chromium content of 12~30% wt) is recognized as an excellent wear-resistant material. The as-cast microstructure of ordinary HCCIs generally consists of eutectic carbide, martensite, and austenite, among others. In white cast iron, the carbon content usually determines its physical and mechanical properties. The high carbon content of cementite and martensite leads to its high hardness and brittleness, which is not conducive to machining. Similarly, austenite has good toughness but low hardness. Therefore, alloying and heat treatment of HCCIs is often performed in industry to optimize their properties [1–5]. At present, sand casting, gravity casting, and squeeze casting are widely used to prepare HCCIs. Compared with the as-cast microstructure, the microstructure of HCCIs prepared using the squeeze casting process is refined and its mechanical performance is improved. The enhanced microstructure and mechanical performance can be attributed to the fact that the pressure used during the squeeze casting process ensures that the casting makes full contact with the mould, increasing its thermal dissipation area and therefore shortening the alloy solidification time. An increase in the alloy cooling rate inhibits atoms such as C, Cr, and Mn, from diffusing, and the grains grow unrestricted, thus refining the crystalline grains [6,7]. Enhancing the crystalline grain growth directly impacts the morphology and quantity of the microstructure, which are key factors in determining its properties [8,9].

The parts of HCCI are usually used in occasions with severe impact, stress concentration and high wear resistance, which makes the materials prone to fatigue failure, so HCCIs are required to have a high hardness and sufficient impact toughness. In order to improve the hardness and toughness of HCCI alloy, many research projects are carrying

out high-temperature heat treatment of HCCIs. For example, Suo et al. [10] conducted heat treatment at approximately 1000 °C on a 20 wt% Cr HCCI with slightly lower carbon content and obtained an alloy with a Rockwell hardness of 56 HRC and an impact toughness of 4.8–5.4 J/cm^2; the performance was improved compared with that of a conventional as-cast, realising the coordination of hardness and toughness. Han et al. [11,12] determined that as the heat treatment temperature increased, both the overall hardness and microhardness increased, until the maximum values were reached at the instability temperature of 1000 °C. Thereafter, the hardness started to decrease as the temperature continued to increase. Although conventional high temperature quenching heat treatment can increase the hardness of HCCIs, their high brittleness makes them susceptible to cracking during the process, which may increase production costs. Therefore, people try to reduce the quenching temperature and explore the subcritical quenching process of HCCI. In the case of researching the subcritical quenching of HCCIs, the fundamentals are often based on the research of gravity die cast HCCIs. Qiang Liu [13] reported that in HCCI alloys containing 15–20 wt% Cr, the secondary carbides are M_7C_3 type, whereas when the Cr content reaches 25–30 wt%, they are $M_{23}C_6$ type. Zhang et al. [14] verified the formation of secondary carbide particles after subcritical heat treatments of two chromium cast irons with different Cr content. Sun et al. [15] studied the effect of subcritical heat treatments on a 16Cr-1Mo-1Cu cast iron using transmission electron microscopy (TEM), noting a certain sequence of secondary carbide formation/transformation in relation to the holding time. K.Wieczerak et al. [16] investigated an in-situ transformation in eutectic carbides from hexagonal M_7C_3 to cubic $M_{23}C_6$ after heating in the rapidly solidified hypoeutectic Fe-Cr-C alloy with a composition of 25Cr-0.8C. However, the influence of the subcritical quenching process on the microstructure, toughness, and hardness of the HCCI alloy prepared via squeeze casting is unknown. To address this problem, this paper aims to explore the subcritical quenching process of the KmTBCr20Mo HCCI prepared via squeeze casting and its composition and microstructure under different quenching temperatures. Furthermore, insights into how the composition and phase content impacts the hardness and impact toughness of HCCIs is revealed.

The process parameters of subcritical quenching usually include the quenching temperature, holding time, and quenching rate. In this study, the heat treatment process of ^{21}Cr HCCI prepared via 128 MPa squeeze casting at different subcritical quenching temperatures was investigated to explore the influence of quenching temperature. Five quenching temperatures were investigated: 500 °C, 530 °C, 550 °C, 580 °C, and 630 °C, along with one control group sample without heat treatment. The six groups of samples were used to observe the evolution of the microstructure by analysing the morphology and content of the matrix microstructure and carbide. The evolution behavior of the microstructure and properties of the alloy with changing subcritical quenching temperature was also investigated.

2. Experimental Procedures

2.1. Experimental Materials and Preparation Methods

The HCCI used for heat treatment research is hypo-eutectic white cast iron with eutectic degree of SC < 1 and carbon equivalent of w (CE) < 4.26%. The exact chemical species used in this study was KmTBCr20Mo (China Brand), which is a complex Fe-Basic alloy based on Fe-C-Si. An M4000 direct reading spectrometer (MIDAC Corporation, Westfield, MA, USA) was used for chemical composition determination, and the results are shown in Table 1. This alloy sample is made by melting and mixing different raw materials. The preparation process of the alloy material is described below.

Table 1. Chemical composition of the HCCI (wt%).

C	Si	Mn	Ni	Cr	Mo	Ti	Cu	B	P	S
3.125	0.675	0.490	0.180	21.412	0.428	0.019	0.080	0.011	<0.02	<0.02

The material preparation process for the heat treatment test sample was divided into three steps. Firstly, the preparation of raw materials included recovered HCCI(KmTBCr20Mo), high-carbon ferromanganese (FeMn74C7.5), high-carbon ferrochrome (FeCr55C10.0), low-carbon ferrochrome (FeCr55C0.25), ferromolybdenum (FeMo55), ferroboron (FeB18C < 0.5), copper plate (Cu), recarburizers (C: FC99 grade), and rare earth silicon (195023). The chemical compositions are shown in Table 2. The second step was smelting. The materials were placed sequentially into a 500 kw medium frequency induction furnace according to a certain mass ratio. The materials were melted and poured into a ladle after reaching a temperature of 1540 °C. The ladle was lined with quartz sand or aluminium-magnesium spinel and was thoroughly baked before use. Finally, the third step comprised of casting. The molten alloy was poured out and an overhead crane scale was used to measure its mass. A certain weight (15kg) of molten steel was quickly poured into the chamber of the liquid forging die. The pouring temperature was 1524 °C, after that, the hydraulic forging machine applies 128MPa pressure to complete the forming process. See Section 2.2 for specific equipment and parameters.

Table 2. Chemical composition of the materials.

Alloys	Chemical Composition (wt%)									
	Mn	**Ni**	**Cr**	**Mo**	**Ti**	**Cu**	**B**	**C**	**Si**	**Re**
KmTBCr20Mo	0.628	0.435	21.718	0.402	0.029	0.087	0.008	3.469	0.579	22.18
195023	2.13				1.53				41.44	22.18
FeMn74C7.5	75.18							6.99	1.61	
FeCr55C10.0			53.01					8.48	0.67	
FeCr55C0.25			55.23					0.21	1.57	
FeMo55				55.01		0.65		0.019	0.58	
FeB18C < 0.5							18.33	0.36	0.35	
C								100		
Cu						100				

2.2. Experimental Equipment and Process

The composite hammer die was installed onto the Y32-630T liquid die forging hydraulic press (Hongkai Heavy Machine Tool Co., LTD., Xingtai, China). The hydraulic press and die structure are shown in Figure 1a,b, and the principle technical parameters of the hydraulic press are shown in Table 3. The upper and lower die structures were used for indirect liquid forging. To obtain the composite hammer casting, the die preheating temperature was set to 220 °C, the pressure was set to 128 MPa, and the holding time was 80 s. Samples were retrieved from the functional part of the hammer head-HCCI and cut into 55 × 10 × 10 mm^3 samples using a wire cutting machine DK7763. The obtained samples were subjected to heat treatment experiments to explore the changes in hardness and impact toughness along with the subcritical quenching temperature. The location and dimensions of the mechanical specimens are given in Figure 1c.

Table 3. Main technical parameters of hydraulic press.

Parameter	Unit	Numerical Value
Nominal force of the master cylinder	kN	6300
Return force	kN	1000
Nominal force of the extrusion bar	kN	1000
Return force of extrusion bar	kN	500
Stroke of extrusion bar	mm	450
Fast-forward speed of the extrusion cylinder	mm/s	100
Lower cylinder nominal force	kN	50
Return force of the lower cylinder	kN	15
Lower cylinder propulsion speed	mm/s	100
Lower cylinder stroke	mm	200

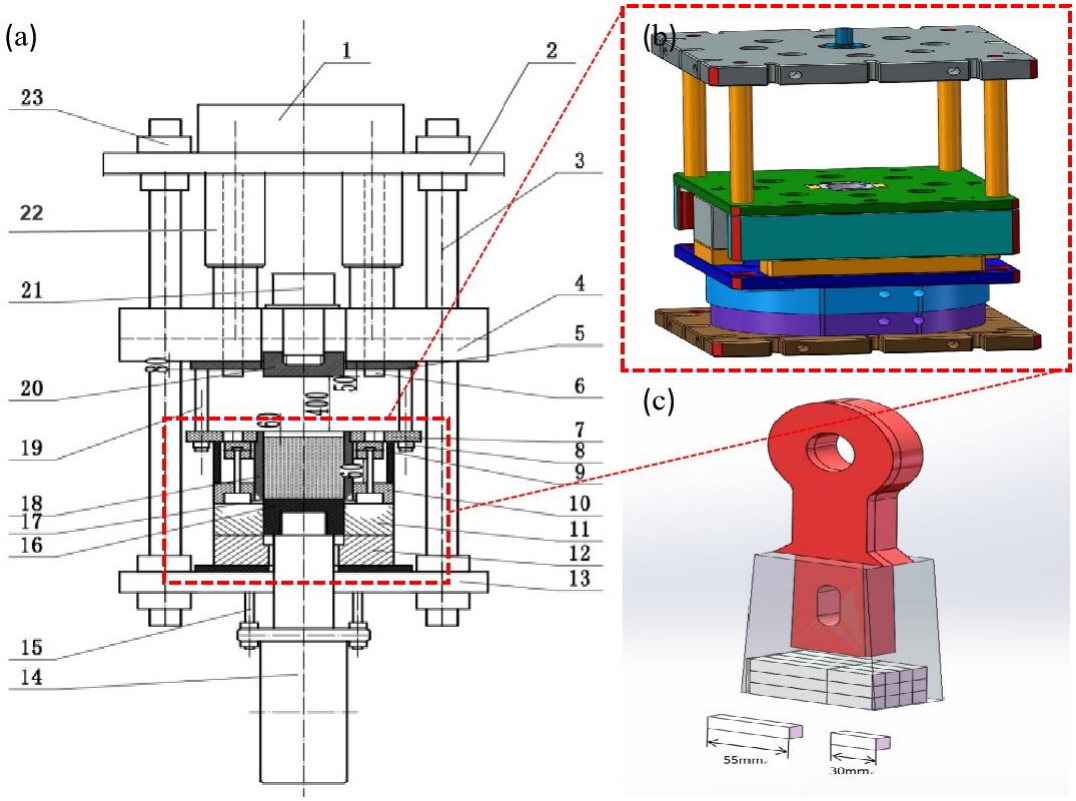


Figure 1. (**a**) Schematic of composite hammer squeeze casting; 1—Hydraulic system; 2—Upper beam; 3—Column; 4—Slider; 5—Bar mounting plate; 6—Push rod; 7—Upper die pressing plate; 8—Lock nut; 9—Upper die sleeve; 10—Upper die; 11—Lower die; 12—Lower die leg; 13—Workbench; 14—Lower head support cylinder; 15—Lower cylinder hanger; 16—Lower head; 17—Workpiece mold cavity; 18—Barrel; 19—Pull rod; 20—Upper ram; 21—Squeeze cylinder; 22—Clamping cylinder; 23—Lock nut; (**b**) Mould structure diagram; (**c**) Location and dimensions of the mechanical specimens.

2.3. Subcritical Quenching Experiment

The samples of dimensions 55 × 10 × 10 mm^3 were checked using visual inspection for dirt, impurities, and for suitable surface flatness. Subsequently, they were numbered for the subcritical quenching test. Two samples were used for each group of experiments to test for reproducibility. A BFX-12B heat treatment resistance furnace (Beijing Freimon Experimental Equipment Co., LTD., Beijing, China) was used to heat the samples, and five quenching temperatures were selected for the experiments. Each sample was placed in the centre of the heat treatment furnace and heated at room temperature. The heating time was 90 min to reach the specified temperature. Thereafter, the samples were subjected to 6 h of heat-preservation, 1.5 h of air cooling, and 12 h of tempering at 150 °C. Finally, the samples were removed for air cooling. The specific heat treatment scheme is shown in Table 4 and a schematic of the heat treatment process flow is shown in Figure 2. The control group, Group JY, did not undergo heat treatment. The samples were polished using an abrasive paper and a diamond spray polishing agent and corroded with 4% nitric acid alcohol solution. Finally, the obtained metallographic specimens underwent hardness and impact toughness measurements.

Table 4. Experimental scheme of subcritical quenching.

Sample	Quenching Temperature/°C	Soaking Time/h	Cooling	Tempering/°C	Soaking Time/h	Cooling
JY500	500	6	Air cooling	150	12	Air cooling
JY530	530					
JY550	550					
JY580	580					
JY630	630					
JY	control group—liquid-forged state					

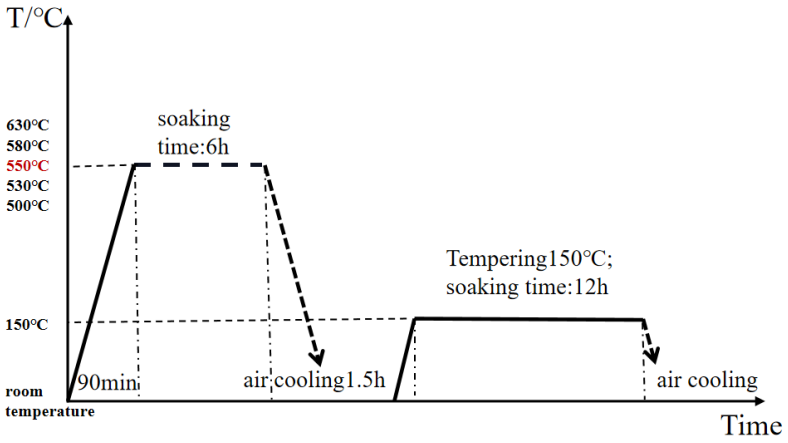


Figure 2. Schematic of heat treatment process flow.

2.4. Analysis Instruments

To characterise the microstructure, the prepared metallographic samples were analysed using an optical microscope (OM, DM2000; Leica Microsystems (Shanghai) Trading Co., LTD., Shanghai, China) and a scanning electron microscope (SEM, TESCANVEGA III, Tokyo, Japan) equipped with energy dispersive spectroscopy (EDS, Oxford, UK). Phase identification of the non-heat treatment group and the 500 °C heat treatment group was performing via X-ray diffraction (XRD) using the D/max-2550 (Rigaku Corporation, Tokyo, Japan). The test step was selected to be 0.02°, 2θ ranged from 5–90°, scanning speed was 5°/min, and the measurements were performed at room temperature. THBRV-187.5 electric Brinell hardness tester (Lab Testing Technology Co., Ltd, Jiashan, China) was used for the hardness test. Three points were considered from each sample, and the distance between each point was chosen to be no less than 3–5 times the indentation diameter. The results of the hardness tests were averaged and taken for further analysis. JB-50 impact testing machine (Jinan Kehui Test Equipment Co., Ltd., Jinan, China) with specification of 25/50 J was used for impact toughness measurements.

3. Experimental Results and Analysis

3.1. Optical Microstructures Analysis

Figure 3 shows the OM images of the squeeze casting HCCI microstructure for the control group and the different heat treatment groups. The black component of the images is the matrix composed of carbide-embedded martensite and retained austenite. The cementite is too hard to be corroded by nitric acid and alcohol solution; therefore it appears as bright white under the microscope. The large phase with rhombic and hexagonal shapes is primary carbide, whereas the small, granular dispersed phase is secondary cementite. The chrysanthemum-like discontinuous phase precipitated from the martensite is eutectic carbide. This coarse eutectic carbide phase network formed directly from the liquid solution is stable and unaffected by the heat treatment (HT) process [17]. It can be seen from Figure 3b that the sizes of the JY500 matrix and the eutectic carbides are relatively uniform, and the distribution of granular secondary carbides in the matrix is also very

uniform. However, the three groups of JY550-JY630 contain a coarse black martensite phase, which is distributed independently, and there are less strengthening secondary carbides embedded in matrix. An abundance of martensite and a deficit of carbide will largely reduce the hardness and toughness of the microstructure. To further analyse the matrix phase and carbides of HCCIs, SEM was employed.

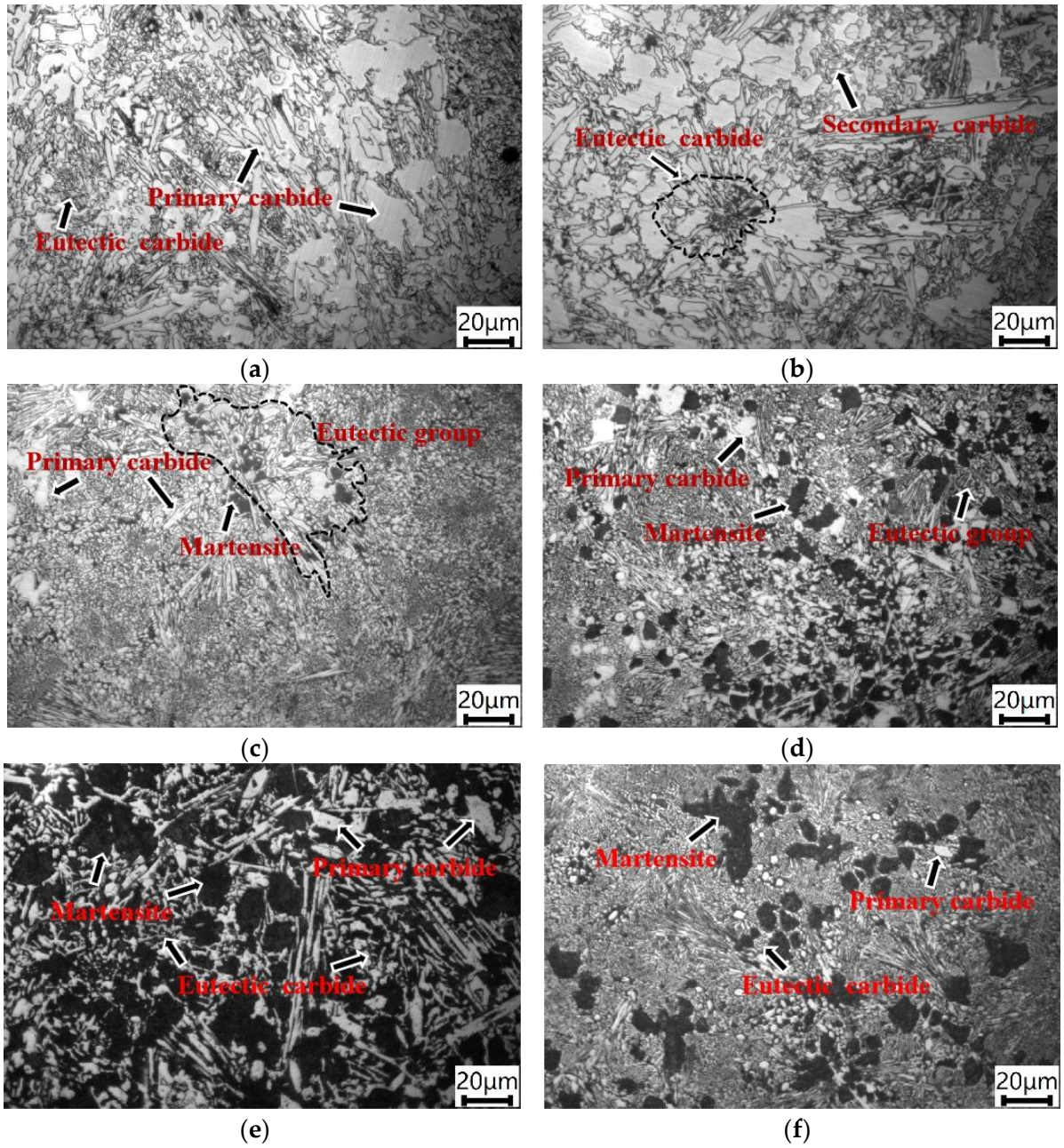


Figure 3. Optical microstructures of the control group and the five groups after subcritical quenching at different temperatures: (**a**) without heat treatment; (**b**) 500 °C-quenching; (**c**) 530 °C-quenching; (**d**) 550 °C-quenching; (**e**) 580 °C-quenching; (**f**) 630 °C-quenching.

3.2. SEM Microstructures Analysis

Figure 4 shows the SEM microstructure images of the control group and the different heat treatment groups. Figure 4a shows that the without heat treatment group has the liquid-forged microstructure that is attributed to a matrix of martensite and retained austenite, a bright white cementite region, and carbides that are distributed on the matrix. The primary

carbides that are distributed in strips and hexagons are unique to HCCIs. While some of the observed hexagonal shapes are regular, there are some hexagonal microstructure boundaries that are rounded. The reasons can be summarised as follows: (1) The large amount of chromium content in this study, the irregular solid–liquid interface of the eutectic crystallisation; and (2) The wide crystallisation area, showing the characteristics of mushy solidification. The hexagonal centre is covered with the secondary cementite produced by the austenitic eutectic reaction. The eutectic carbide tends to grow in a small plane, that is, the carbide grows in the shape of the chrysanthemum, as shown in the figure. Compared with the eutectic cementite in the shape of a plate in the ordinary white cast iron, the carbide in this microstructure is more conducive to improving the hardness and wear resistance of materials.

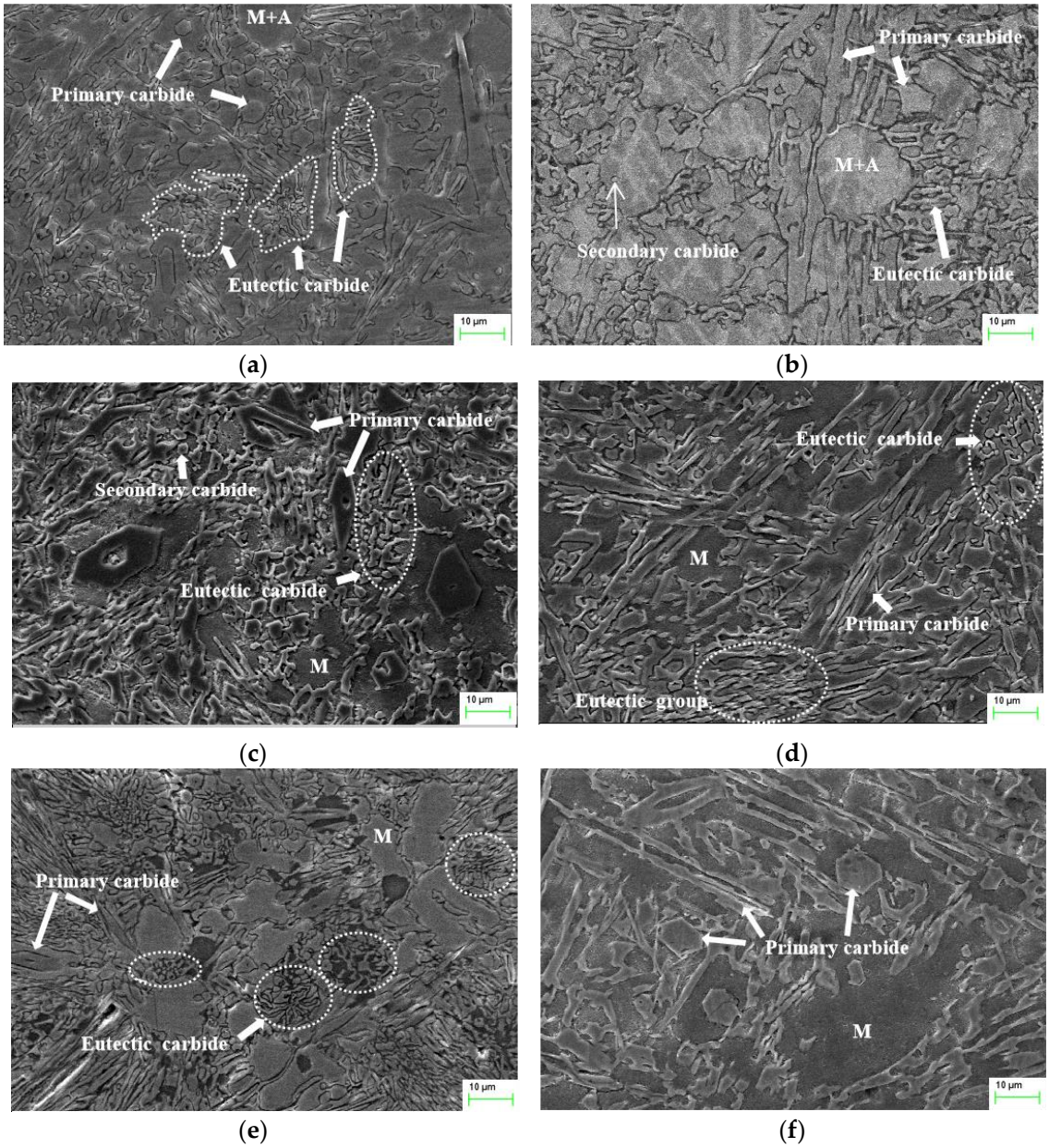


Figure 4. SEM micrographs of the control group and the five groups after subcritical quenching at different temperatures: (**a**) without heat treatment; (**b**) 500 °C-quenching; (**c**) 530 °C-quenching; (**d**) 550 °C-quenching; (**e**) 580 °C-quenching; (**f**) 630 °C-quenching.

It can be seen from Figure 4b that the microstructure of the HCCI significantly changed after heat preservation at 500 °C followed by tempering. First, a large martensite matrix with a uniform size was observed, as shown by the dark gray microstructure in the figure, and the fine granular secondary carbides decomposed from the austenite were uniformly distributed in the matrix. The secondary carbides play a critical role in the dispersion strengthening of the alloy; therefore, the hardness and toughness of the matrix were improved. When compared with the control group, the size of the carbide increased, and it was distributed at the martensite interface intermittently, as shown in Figure 4b. According to the amount of Cr element addition, it was preliminarily determined that the carbide type is M_7C_3, which is a $(Fe, Cr)_7C_3$ carbide. This class of carbide has a relatively high hardness, and therefore, it improves the wear resistance of the matrix.

After heat preservation at 530 and 550 °C followed by tempering, the microstructure of the HCCIs are shown in the Figure 4c,d. The matrix is composed of furious tempered martensite and a small amount of retained austenite, and it is determined that the content of martensite is more than that of the JY500 group. The white strip and block microstructures are identified as primary carbides, which are disorderly distributed within the matrix. Because of their sharp shape and disordered distribution, such carbides easily cut the matrix and introduce structural defects, resulting in higher hardness and brittleness, thereby having adverse effects on the impact abrasive wear. Likewise, in the JY550 group, a eutectic cluster and grain boundary carbide existed in an irregular, small particle shape, with a chaotic microstructure distribution.

After heat preservation at 580 and 630 °C followed by tempering, the microstructure of the HCCIs are shown in Figure 4e,f. As the heating temperature increased, the cooling rate decreased, yielding a coarse and overabundant martensite matrix. The bar and block carbides were scattered along the matrix. When subjected to wear and impact, these isolated carbides easily break off, leading to a substantial decrease in microstructure, ultimately worsening the fracture toughness. Small cracks were distributed on the coarse lath-like and diamond-like primary carbides and the eutectic carbides were sharp, needle-like, and small in shape. The eutectic carbides can easily scratch the matrix, implying that the alloy is highly brittle.

3.3. Hardness Analysis

The hardness test data is shown in Figure 5. The hardness of the HCCI alloy was significantly improved when the subcritical quenching temperature was set to 500, 530, and 550 °C, attaining hardness values of 55, 57, and 55.5 HRC, respectively. However, when the quenching temperatures were set to 530 and 550 °C, the toughness of the sample degraded rapidly, and the impact toughness reduced by a factor of 2. The SEM image analysis of the JY530 and JY550 species revealed that the carbides of the eutectic cluster and grain boundary were irregular in shape, the primary carbide possessed a sharp shape and a disorderly distributed microstructure, and the martensite matrix was coarse, resulting in a significantly reduced impact toughness. In general, except for the 630 °C quenching sample, the alloy's hardness was improved compared with that of the control group without heat treatment. Therefore, it can be determined that subcritical quenching heat treatment can improve the hardness of the alloy of the liquid forged HCCI to a certain extent. However, the hardness increases with the increase in quenching temperature (QT) rather than monotonically. The general changing trend of hardness is that as the quenching temperature increased from 500 to 530 °C, the hardness increased significantly. By contrast, when the quenching temperature continued to rise from 530 to 630 °C, the hardness decreased rapidly.

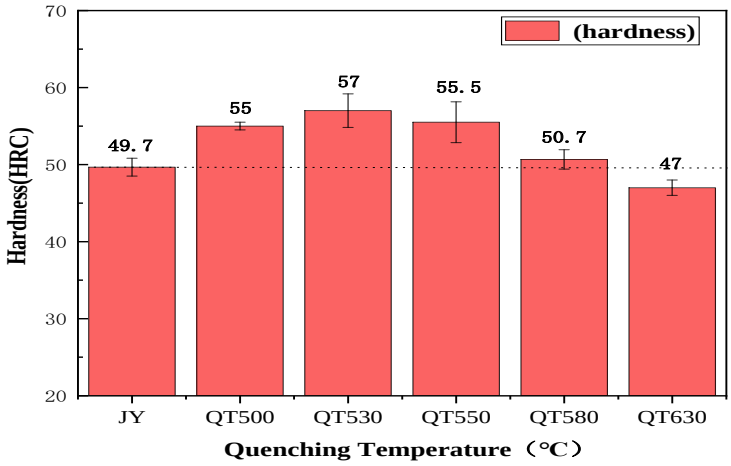


Figure 5. Hardness of HCCI samples treated at different quenching temperatures.

3.4. Impact Toughness Analysis

The impact toughness test data is shown in Figure 6. The HCCI at the subcritical quenching temperature of 500 °C displayed the best toughness, with a value of 7.2 J/cm^2. When the quenching temperature continued to rise, the impact toughness reduced notably to a value approximately 2 times lower than that of the control group without heat treatment. According to the microstructure analysis, the carbides shown in Figure 4a,b were distributed intermittently and had uniform size. Additionally, the fine granular secondary carbides were evenly distributed in the more martensitic matrix, providing dispersion strengthening and therefore yielding relatively high hardness and toughness values. However, when the quenching temperature was 550 °C, the matrix and carbide phases were both coarse and irregular, indicating low toughness. When the quenching temperature was 580 °C, the impact toughness reached a small maximum. According to the results shown in Figures 3e and 4e, the more meshed eutectic carbide M_7C_3 precipitated at the martensite boundary was helpful to improve the impact toughness. In general, it can be concluded that only the 500 °C subcritical quenching can improve the toughness, and continuous heating will substantially reduce the impact toughness.

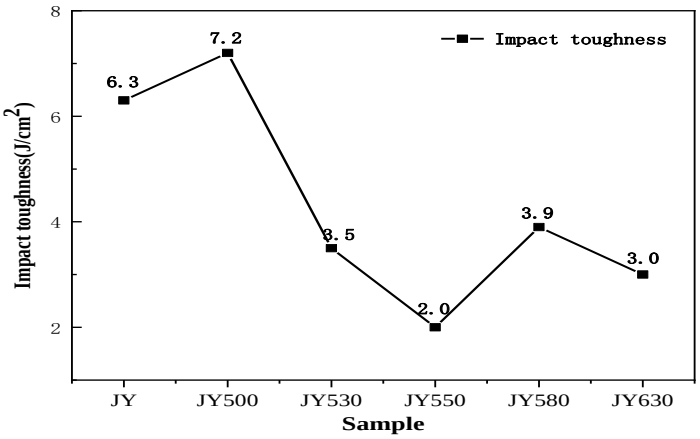
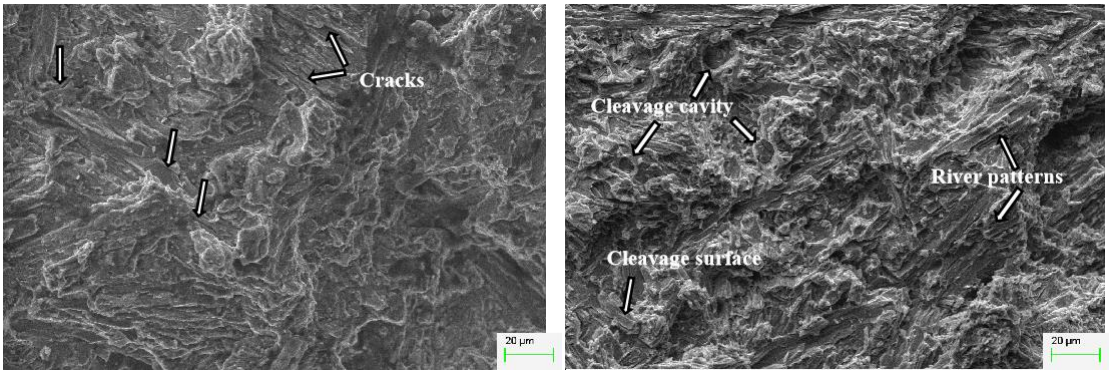


Figure 6. Impact toughness of HCCI samples treated at different quenching temperatures.

Figure 7 shows the SEM micrograph of the impact fracture of the JY630 and JY500 samples. Although both fractures are cleavage or brittle fractures, there are some notable differences. A cleavage fracture is defined as a transgranular fracture along a specific crystal plane. Because the orientation of adjacent grains is different, when the cleavage plane extends from one grain to an adjacent grain, a river pattern, namely the cleavage

step, is formed at the interface. The JY630 fracture cleavage surface is relatively large and many cracks are initiated, as shown in Figure 7a. According to the analysis in Figure 4f, the matrix and the carbide are both large; when impacted, the brittle carbide first breaks and the crack propagates along the carbide in the matrix, eventually leading to sample fracture. By contrast, the fracture of JY500 has a small size cleavage surface, an obvious river pattern, few microcracks, and many cleavage caves, which are created by the falling of small carbide particles. Furthermore, it is known from the microstructure analysis that the carbide is evenly distributed within the matrix, garnering some protection for the matrix. Therefore, when impacted, the carbides relieve some of the stress concentration, limiting the ability of the cracks to expand outward [18]. The improvement of impact toughness primarily depends on the ability to resist crack growth [19]; thus, it can be concluded that the impact toughness of the JY500 is relatively high.

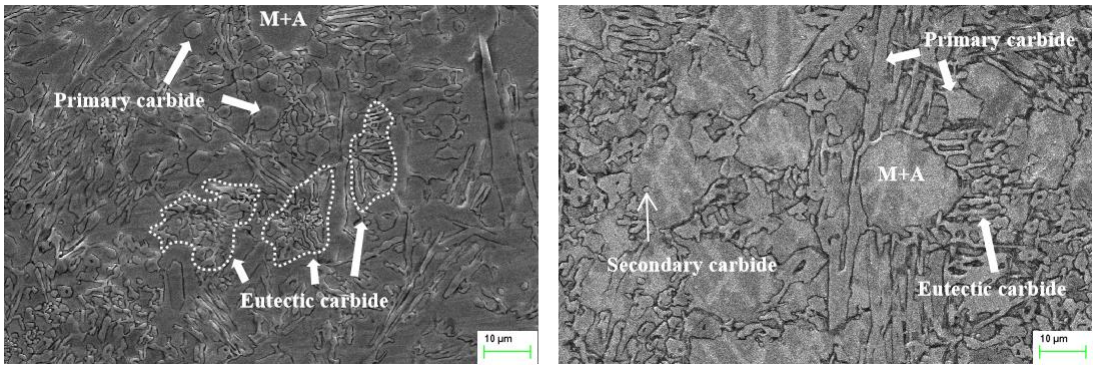


(**a**) (**b**)

Figure 7. Impact fracture of JY630 and JY500 observed using the scanning electron microscope after. (**a**) 630 °C-quenching; (**b**) 500 °C-quenching.

3.5. Discussion on Optimum Subcritical Quenching Temperature

According to the above analysis and detection, when the subcritical quenching temperature is 500 °C, the hardness and impact toughness of the alloy is optimised. Subsequently, we compared the liquid-forged microstructure with the 500 °C-quenched microstructure to further study the microstructure state yielding the best performance and the mechanism of heat treatment to change its microstructure. First, it was obvious from Figure 8, the matrix composed of martensite and retained austenite was significantly increased in the heat treatment group compared to that in the liquid-forged group. More granular secondary carbides were precipitated in the matrix of the heat treated group, which plays a role in dispersion strengthening and can also improve the hardness of the alloy. Second, the eutectic carbide in the liquid-forging state was distributed in a small area of mesh and in a chrysanthemum shape while the size of eutectic carbide after the heat treatment at 500 °C increased and was more evenly distributed on the martensite matrix with no obvious boundary between them. The size and distribution of this carbide play a good role in protecting the matrix, improving the hardness and toughness of the matrix. Because the type and quantity of the carbides are key factors affecting the microstructure and properties of HCCI, the origins of the M_7C_3 type carbides were deeply explored and it was determined that the source primarily included the primary carbide, eutectic carbide, and some of the secondary carbides. The types of secondary carbides may include $M_{23}C_6$, M_3C, and M_6C, among others. The M_7C_3 carbide in the liquid forging state was small, relatively low in abundance, and unevenly distributed, whereas the M_7C_3 carbide after the heat treatment at 500 °C increased in size, quantity, and even in the matrix, allowing the formation of a good, high-strength and ductile microstructure.



(**a**) (**b**)

Figure 8. SEM micrographs of HCCI: (**a**) As-cast; (**b**) Quenching temperature 500 °C.

Further analyses were performed on the clear blocky carbides observed in the group pictures of Figure 8b, and these results are shown in Figure 9. EDS point scanning was carried out at Points 1, 2, and 3 to determine the elemental content. The phases at Points 1 and 2 are martensite, where the dark gray region has a higher C content than the white region. According to the elemental analysis conducted at Point 3, it can be determined that the hexagonal block phase is the M_7C_3 carbide. The distribution and aggregation of the elements can be seen from the surface scanning measurements (The error range of element content was shown in the figure). Notably, the distribution of element C is relatively uniform in the matrix. When C combined with the alloy elements, it formed the carbide M_7C_3 and smaller secondary carbides, including $M_{23}C_6$ and M_7C_3. The remaining C was dissolved in the martensite matrix to improve the hardenability of the matrix. It can also be seen from the distribution of Cr elements in the figure that most of the Cr and C elements converge to form chromium-containing carbides with high hardness [17,20,21], such as M_7C_3 type carbides, and the remainder is also soluble in the matrix to improve the hardenability of the matrix. Furthermore, partial S aggregates in the matrix, whereas Fe is mainly distributed in the matrix as a matrix element.

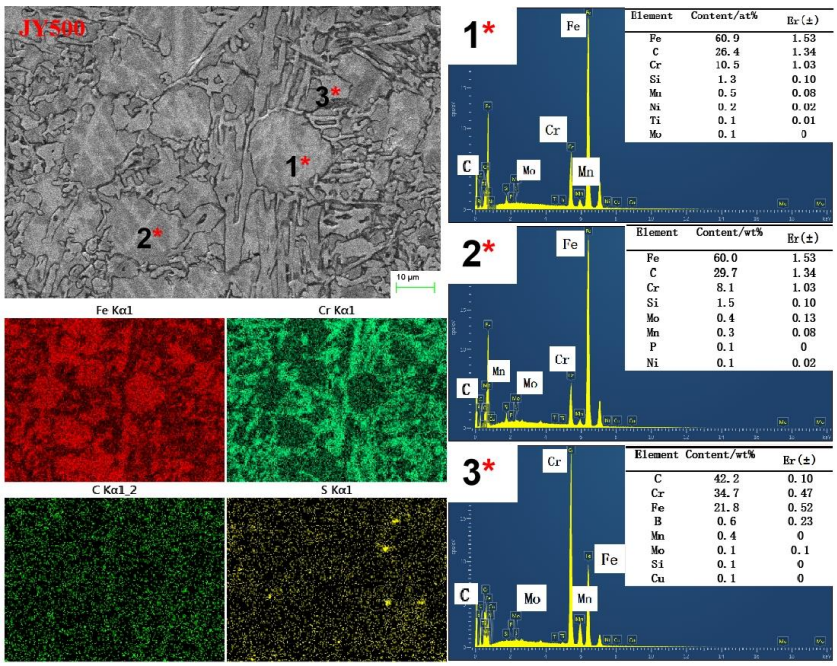


Figure 9. Microstructure and composition of subcritical quenching at 500 °C: EDS point analysis of point A; EDS area scans.

The liquid-forged microstructure and the 500 °C subcritical-quenched microstructure were tested and analysed via X-ray diffraction, and the results are shown in Figure 10. The results obtained from XRD are consistent with the OM and SEM analysis results. The phase composition of the HCCI prepared at 128 MPa specific pressure includes the matrix composed of martensite and austenite, the primary and eutectic M_7C_3 type carbides, some cementite and secondary cementite. However, after reaching the 500 °C subcritical quenching, the phase composition of the microstructure changes. First, the matrix martensite increases, with a small amount of retained austenite, and the types of carbides also increase. In addition to the M_7C_3 type carbides, there are also diffraction peaks characteristic of secondary precipitated carbides $M_{23}C_6$. After further testing, it was found that Fe_3C, Fe_2C, and other carbides are also present in the samples.

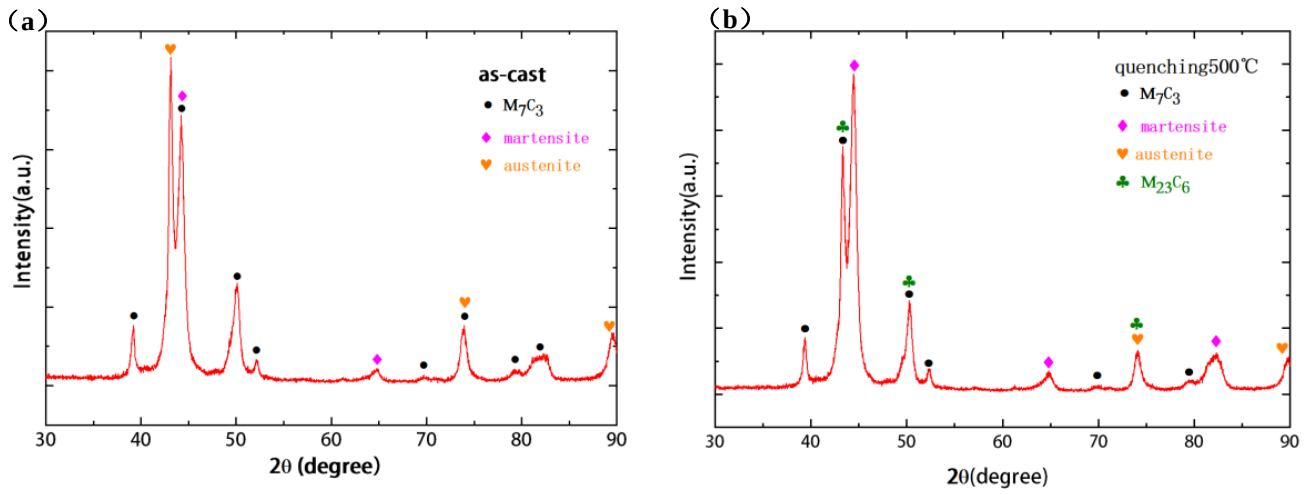


Figure 10. X-ray diffraction determines the phase composition of microstructure: (**a**) As-cast; (**b**) Quenching temperature 500 °C.

In summary, the mechanism of subcritical quenching heat treatment to improve the properties of HCCI can be reduced to two points. First, subcritical quenching heat treatment increases the content of martensite in the matrix and affects the size, morphology, and distribution of the martensite. Tough martensite improves the hardness of the matrix. Second, subcritical heat treatment can change the morphology, quantity, and distribution of the eutectic carbide and the primary carbide M_7C_3, which can directly affect the hardness and toughness of the microstructure. According to OM and SEM microstructure analysis and performance test results, when the quenching temperature is 500 °C, the martensite matrix is refined and the size and distribution is uniform. At this temperature, the carbides are mainly M_7C_3 type carbides with intermittent block distribution and eutectic carbides; the precipitated secondary phase is uniformly distributed in the matrix. Therefore, this analysis is consistent with the testing results of hardness and impact toughness. Among the five groups of quenching processes, 500 °C subcritical quenching is the best one.

Based on the above analysis, the microstructure evolution diagram of the 500 °C optimal subcritical quenching process is constructed. From Figure 11a, the HCCI microstructure prepared via 128 MPa squeeze casting is primarily composed of austenite, the martensite matrix, eutectic carbide, and other carbides. During heating and insulation at 500 °C, the partial coarse carbide phase dissolves, and the C atoms in the carbide are dissolved into the austenitic matrix. At high temperatures, the squeezed C atom can fit into the Fe atom gap of the austenite and experiences some solubility. However, when cooling occurs, the solubility of the C atom decreases. As the C cannot escape from the Fe atom gap, martensite shearing occurs. Simultaneously, when the chromium content exceeds 18–20%, the austenite decomposes into chromium ferrite and carbide [3,22]; therefore, the austenite transforms into secondary cementite. During the entire process, the austenite decreases,

the martensite increases, the types of carbides increase, and the size of the eutectic carbides also increases. At the end of the final cooling, the phase composition becomes the matrix comprised of the martensite and retained austenite, eutectic carbide growing along the martensite matrix, secondary cementite, primary carbide, and other types of carbides.

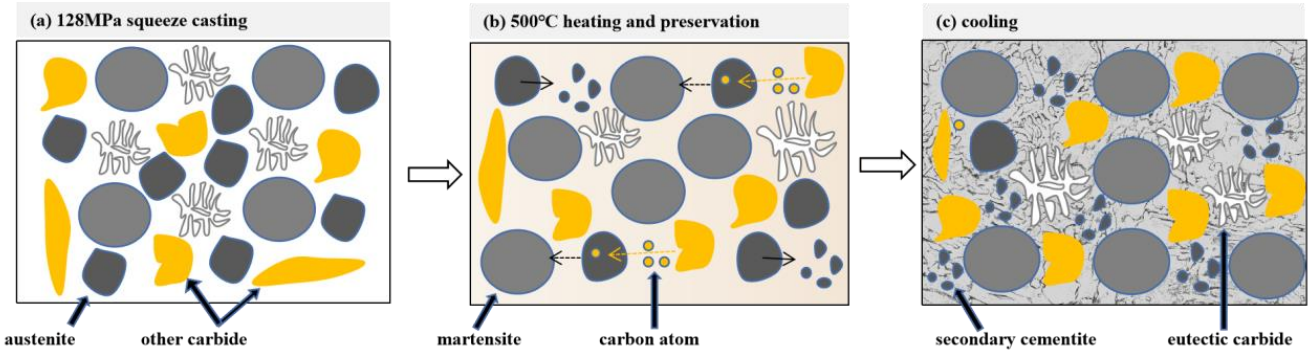


Figure 11. Microstructure evolution diagram of 500 °C subcritical quenching process: (**a**) microstructure of 128 Mpa squeeze casting HCCI without heat treatment, (**b**) phase transformation diagram of extruded HCCI during 500 °C heating and preservation, (**c**) final phase diagram after heat treatment and cooling.

4. Conclusions

In this study, the following conclusion could be drawn:

The subcritical quenching heat treatment process can change the morphology, size, and quantity of the squeeze casting HCCI microstructure. It was determined that this phenomenon primarily arose owing to an increase in the martensite matrix, producing more M_7C_3 type carbides and enriching the types of carbides. Compared with the liquid-forged martensite matrix, the samples quenched at 500 °C possessed a more regular size. The matrix precipitates dispersed granular secondary carbides, while the size of the eutectic carbide and M_7C_3 carbide distributed in strips and hexagonal blocks increased, and the hardness and toughness significantly improved. When the quenching temperatures were 530 and 550 °C, the martensite phase increased, and the size difference of the JY530 carbide was too large, as the JY550 carbide structure consisted of a sharp needle and bar shape, resulting in high hardness and low toughness. When the quenching temperatures were 580 and 630 °C, there was an overabundance of martensite content causing the shape to be coarse, while the carbide exhibited an acicular distribution. Among the carbides, the JY580 group contained more network eutectic carbide, which helped improve the alloy toughness.

The subcritical quenching heat treatment can improve the hardness of the alloy of squeeze casting HCCI. When the quenching temperature rose from 500 to 530 °C, the hardness of the alloy increased significantly. If the temperature continued to rise to 630 °C, the hardness decreased rapidly. In general, except for 630 °C quenching, the samples' hardness of the other heat treatment groups improved compared with that of the control group. In other words, subcritical quenching heat treatment can improve the alloy hardness to a certain extent.

The subcritical quenching heat treatment can change the impact toughness of the squeeze casting HCCI. When the quenching temperature was 500 °C, the alloy's toughness increased by 0.9 J/cm^2 compared with that of the control group. With the continuous increase in quenching temperature, the toughness of the alloy decreased significantly.

When the quenching temperature was 530 °C, the hardness reached a maximum but the toughness was only 3.5 J/cm^2. When the quenching temperature was 500 °C, the impact toughness was the highest, reaching 7.2 J/cm^2. Concurrently, the hardness was also 5.3 HRC higher than that of the control group, reaching 55 HRC. Therefore, by balancing the need for both optimised hardness and impact toughness, the best subcritical quenching

temperature was selected to be 500 °C. Compared with high temperature heat treatment, subcritical heat treatment can not only improve the performance of HCCI alloys, but also reduce the production cost and bring huge economic benefits for relevant industries.

Author Contributions: Conceptualization, A.S., S.X. and B.Z.; formal analysis, H.S.; investigation, W.G.; resources, T.W.; writing—original draft preparation, A.S.; writing—review and editing, A.S. and S.X. All authors have read and agreed to the published version of the manuscript.

Funding: This research was funded by the Fundamental Research Funds for the Central Universities under Grant No. 2020YJS146.

Data Availability Statement: Data will be made available on request.

Conflicts of Interest: The authors declare no conflict of interest.

References

1. Kadowaki, M.; Muto, I.; Katayama, H.; Masuda, H.; Sugawara, Y.; Hara, N. Effectiveness of an intercritical heat-treatment on localized corrosion resistance at the microstructural boundaries of medium-carbon steels. *Corros. Sci.* **2019**, *4*, 19. [CrossRef]
2. Hadji, A.; Bouhamla, K.; Maouche, H. Improving wear properties of High-Chromium Cast Iron by manganese alloying. *Int. J. Metalcast.* **2016**, *10*, 43–55. [CrossRef]
3. Wang, J.; Xiong, J.; Fan, H.; Yang, H.-S.; Liu, H.-H.; Shen, B.-L. Effects of high temperature and cryogenic treatment on the microstructure and abrasion resistance of a high chromium cast iron. *J. Mater. Process. Technol.* **2009**, *209*, 3236–3240. [CrossRef]
4. Gelfi, M.; Pola, A.; Girelli, L.; Zacco, A.; Masotti, M.; La Vecchia, G.M. Effect of heat treatment on microstructure and erosion resistance of white cast irons for slurry pumping applications. *Wear* **2019**, *428*, 438–448. [CrossRef]
5. Tabrett, C.P.; Sare, R.; Ghomashci, R. Microstructure-property relationships in high chromium white iron alloys. *Int. Mater. Rev.* **1996**, *41*, 59–82. [CrossRef]
6. Souissi, S.; Ben Amar, M.; Bradai, C. Microstructure characterization and tensile properties of direct squeeze cast and gravity die cast 2017A wrought Al alloy. *Int. J. Mater. Form.* **2011**, *6*, 249–254. [CrossRef]
7. Hajjari, E.; Divandari, M. An investigation on the microstructure and tensile properties of direct squeeze cast and gravity die cast 2024 wrought Al alloy. *Mater. Des.* **2008**, *29*, 1685–1689. [CrossRef]
8. Jain, A.-S.; Chang, H.; Tang, X.; Hinckley, B.; Zhang, M.-X. Refinement of primary carbides in hypereutectic high-chromium cast irons: A review. *J. Mater. Sci.* **2021**, *56*, 999–1038. [CrossRef]
9. Wu, X.; Xing, J.; Fu, H.; Zhi, X. Effect of titanium on the morphology of primary M7C3 carbides in hypereutectic high chromium white iron. *Mater. Sci. Eng. Proc. Conf.* **2007**, *457*, 180–185. [CrossRef]
10. Suo, Z.Y.; Fu, L.M.; Zhang, Z.H.; Wang, Y.J.; Shan, A.D. Influence of heat treatment on microstructure and properties of Cr20 high chromium cast iron. *Heat Treat. Met.* **2018**, *43*, 184–187. (In Chinese)
11. Han, Y.J.; Zhi, X.H.; Guo, W.W.; Xing, Y.M. Influence of heat-treatment on the microstructure and properties of hypereutectic high-chromium cast iron containing Ti. *Rare Met. Mater. Eng.* **2010**, *39*, 142–145.
12. Chen, C.L.; Feng, A.X.; Liu, B.J.; Wei, Y.C.; Song, X.Y. Effect of quench-tempering and laser quenching on the microstructure and properties of high-chromium cast iron. *J. Mater. Res. Technol.* **2022**, *19*, 2759–2773. [CrossRef]
13. Liu, Q.; Shibata, H.; Hedström, P.; Jönsson, P.G.; Nakajima, K. Dynamic precipitation behavior of secondary M7C3 carbides in Ti-alloyed high chromium Cast Iron. *ISIJ Int.* **2013**, *53*, 1237–1244. [CrossRef]
14. Zhang, M.X.; Kelly, P.M.; Gates, J.D. The effect of heat treatment on the toughness hardness and microstructure of low carbon white cast irons. *J. Mater. Sci.* **2001**, *36*, 3865–3875. [CrossRef]
15. Sun, Z.; Zuo, R.; Li, C.; Shen, B.; Yan, J.; Huang, S. TEM study on precipitation and transformation of secondary carbides in 16Cr-1Mo-1Cu white iron subjected to subcritical treatment. *Mater. Charact.* **2004**, *53*, 403–409. [CrossRef]
16. Wieczerzak, K.; Bala, P.; Dziurka, R.; Tokarski, T.; Cios, G.; Koziel, T.; Gondek, L. The effect of temperature on the evolution of eutectic carbides and M7C3 → M23C6 carbides reaction in the rapidly solidified Fe-Cr-C alloy. *J. Alloys Compd.* **2017**, *698*, 673–684. [CrossRef]
17. Oanh, N.T.H.; Viet, N.H. Precipitation of M23C6 Secondary Carbide Particles in Fe-Cr-Mn-C Alloy during Heat Treatment Process. *Metals* **2020**, *10*, 157. [CrossRef]
18. Li, Y.; Li, P.; Wang, K.; Li, H.; Gong, M.; Tong, W. Microstructure and mechanical properties of a Mo alloyed high chromium cast iron after different heat treatments. *Vacuum* **2018**, *156*, 59–67. [CrossRef]
19. Huang, Z.; Xing, J.; Gao, Y.; Zhi, X. Effect of titanium on the as-cast microstructure and impact toughness of hypereutectic high-chromium cast iron. *Int. J. Mater. Res.* **2012**, *103*, 609–612. [CrossRef]
20. Das, R.; Ray, K.K.; Chakrabarti, A.K. Semisolid heat treatment of chromium cast iron. *Int. J. Cast Met. Res.* **2006**, *19*, 130–133. [CrossRef]

21. Wiengmoon, A.; Pearce, J.T.H.; Chairuangsri, T. Relationship between microstructure, hardness and corrosion resistance in 20wt.%Cr, 27wt.%Cr and 36wt.%Cr high chromium cast irons. *Mater. Chem. Phys.* **2011**, *125*, 739–748. [CrossRef]
22. Siekaniec, D.; Kopyciński, D.; Tyrała, E.; Guzik, E.; Szczęsny, A. Optimisation of Solidification Structure and Properties of Hypoeutectic Chromium Cast Iron. *Materials* **2022**, *15*, 6243. [CrossRef] [PubMed]

Disclaimer/Publisher's Note: The statements, opinions and data contained in all publications are solely those of the individual author(s) and contributor(s) and not of MDPI and/or the editor(s). MDPI and/or the editor(s) disclaim responsibility for any injury to people or property resulting from any ideas, methods, instructions or products referred to in the content.